New Homoleptic Organometallic Derivatives of Vanadium(III) and Vanadium(IV): Synthesis, Characterization, and Study of Their Electrochemical Behaviour

Pablo J. Alonso, Juan Forniés, M. Angeles García-Monforte, Antonio Martín, and Babil Menjón*[a]

Abstract: The arylation of $[VCl_3(thf)_3]$ with LiR_{Cl}, where R_{Cl} is a polychlorinated phenyl group [C_6Cl_5, 2,4,6-trichlorophenyl(tcp), or 2,6-dichlorophenyl (dcp)] gives four-coordinate, homoleptic organovanadium(III) derivatives with the formula $[Li(thf)_4][V^{III}(R_{Cl})_4]$ (R_{Cl} = C_6Cl_5 (**1**), tcp (**2**), dcp (**3**)). The anion $[V^{III}(C_6Cl_5)_4]^-$ has an almost tetrahedral geometry, as observed in the solid-state structure of $[NBu_4][V(C_6Cl_5)_4]$ (**1′**) (X-ray diffraction). Compounds **1**–**3** are electrochemically related to the neutral organovanadium(IV) species $[V^{IV}(R_{Cl})_4]$ (R_{Cl} = C_6Cl_5 (**4**), tcp (**5**), dcp (**6**)). The redox potentials of the V^{IV}/V^{III} semisystems in CH_2Cl_2 decrease with decreasing chlorination of the phenyl ring ($E_{1/2}$ = 0.84 (**4**/**1**), 0.42 (**5**/**2**), 0.25 V (**6**/**3**)). All the $[V^{IV}(R_{Cl})_4]$ derivatives involved in these redox couples could also be prepared and isolated by chemical methods. The arylation of $[VCl_3(thf)_3]$ with LiC_6F_5 also gives a homoleptic organovanadium(III) compound, but with a different stoichiometry: $[NBu_4]_2[V^{III}(C_6F_5)_5]$ (**7**). In this five-coordinate species, the C_6F_5 groups define a trigonal bipyramidal environment for the vanadium atom (X-ray diffraction). EPR spectra for the new organovanadium compounds **1**–**6** are also given and analysed in terms of an elongated tetrahedral structure with C_{2v} local symmetry. It is suggested that the R_{Cl} groups exert a protective effect towards the vanadium centre.

Keywords: cyclic voltammetry · EPR spectroscopy · homoleptic compounds · open-shell compounds · vanadium

Introduction

"Unless supported by cyclopentadienyl ligands, […] vanadium(III) alkyls and aryls remain rare". This statement can be read in a comprehensive review on the organometallic chemistry of vanadium and is still valid today.[1] Even rarer, however, are those organovanadium(III) derivatives in which a given alkyl or aryl group R is the only ligand coordinated to the metal and hence solely responsible for the stability of the complex species. These homoleptic σ-organyl compounds[2] are of fundamental interest and should have the general formula $[VR_n]^{(n-3)-}$, n being a small integer. As far as we know, the only stoichiometries for which homoleptic σ-organovanadium(III) derivatives have been isolated to date are $[VR_4]^-$ (R = 2,4,6-trimethylphenyl (mes),[3] 2-methylphenyl[4] or 2,6-dimethoxyphenyl[5]) and $[VR_3]$ (R = mes[6] or $CH(SiMe_3)_2$[7]), with no unequivocal structural information available for any of them. The neutral compound $[V\{C(CN)_3\}_3]$ was assigned a polymeric structure based on octahedral VN_6 motifs and so cannot be regarded as an organometallic derivative.[8] In fact, the coordination behaviour of the tricyanomethanide anion, despite its formula, $[C(CN)_3]^-$, bears a greater resemblance to a triple nitrile than to an organyl group—as documented in several other transition-metal derivatives.[9]

Further to a previous communication,[10] we now report on a series of electrochemically related couples of organovanadium compounds $[V^{IV}(R_{Cl})_4]/[V^{III}(R_{Cl})_4]^-$, where R_{Cl} is a polychlorophenyl group (C_6Cl_5, 2,4,6-trichlorophenyl (tcp),

[a] Prof. Dr. P. J. Alonso, Prof. Dr. J. Forniés, Dr. M. A. García-Monforte, Dr. A. Martín, Dr. B. Menjón
Instituto de Ciencia de Materiales de Aragón
Facultad de Ciencias, Universidad de Zaragoza–C.S.I.C.
C/Pedro Cerbuna 12, 50009 Zaragoza (Spain)
Fax: (+34) 976-761-187
E-mail: menjon@unizar.es

Supporting information for this article is available on the WWW under http://www.chemeurj.org/ or from the author. It contains experimentally measured and calculated EPR spectra of **1**, **1′**, **2** and **3**, as well as the procedure used to derive the spin-Hamiltonian parameters of the $[V^{III}R_4]^-$ systems (R = C_6Cl_5, 2,4,6-trimethylphenyl) from their optical absorption spectra.

 DOI: 10.1002/chem.200401190

or 2,6-dichlorophenyl (dcp)). The characterisation of these paramagnetic (d^1/d^2) species includes a detailed EPR study. Finally, the use of the C_6F_5 ligand has allowed us to obtain the $[VR_5]^{2-}$ stoichiometry, unprecedented in organometallic chemistry.

Results and Discussion

Synthesis and structural characterisation of the $[V^{III}(R_{Cl})_4]^-$ salts: The arylation of $[VCl_3(thf)_3]$ with different LiR_{Cl} reagents in Et_2O at −78 °C, followed by appropriate treatment, enabled us to obtain the compounds $[Li(thf)_4][V^{III}(R_{Cl})_4]$ (R_{Cl} = C_6Cl_5 (**1**), tcp (**2**), dcp (**3**)) as highly hygroscopic, green solids in moderate to poor yields (Scheme 1).

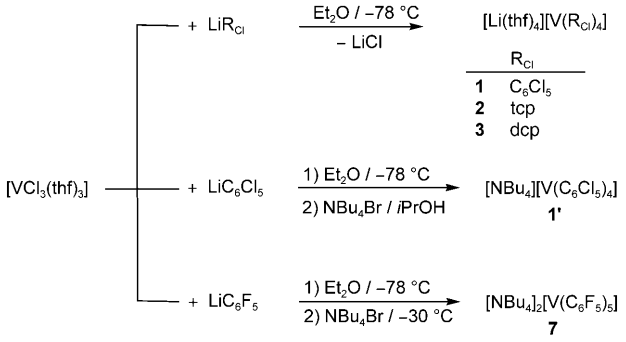

Scheme 1. Production of the homoleptic arylvanadate(III) compounds **1**–**3**, **1′**, and **7**.

These compounds were characterised by using analytical and spectroscopic methods.

The mass spectra (FAB^-) of compounds **1**–**3** all contain the peaks associated with the corresponding $[V(R_{Cl})_4]^-$ anions, together with several fragments of general formula $[V(R_{Cl})_{4-n}Cl_n]^-$ resulting from the sequential replacement of R_{Cl} groups by Cl atoms. Some other fragments could also occasionally be observed, and these were easily related to the parent $[V(R_{Cl})_4]^-$ species by different degradation processes. In no case were peaks that might suggest the coordination of thf to vanadium observed.

The IR spectra of compounds **1**–**3** contain absorptions attributable to the symmetric and asymmetric stretching modes of the C−O−C unit (ether link) in the thf molecule.[11] The IR spectrum of **1** also contains the characteristic absorptions of the metal-coordinated C_6Cl_5 group, the most significant of which is the X-sensitive mode appearing at 829 cm^{-1}.[12] No absorption could be assigned to the ν(M−C) mode. The lack of appropriate spectroscopic studies involving the tcp and dcp groups makes the IR spectra of compounds **2** and **3** less useful, though they still retain their fingerprint function.

The formulation suggested for compounds **1**–**3**, in which all four thf molecules are bound to the Li^+ cation with no coordination of any of them to the V^{III} centre, was supported by cation-exchange experiments. Thus, addition of NBu_4Br to solutions of **1** in *i*PrOH allowed $[NBu_4][V^{III}(C_6Cl_5)_4]$ (**1′**) to be obtained in moderate yield (Scheme 1). This salt behaves as a 1:1 electrolyte in acetone (Λ_M = 108.1 $S\,cm^2\,mol^{-1}$)[13] and, in contrast with the hygroscopic character of its parent species **1**, complex **1′** is air- and moisture-stable. The IR and mass spectra of **1′** show features similar to those just discussed for **1**, except for the peaks and absorptions due to the cation.

The crystal structure of **1′** was determined by using X-ray diffraction methods. As far as we know, this is the first structural characterisation of a homoleptic σ-organovanadium(III) compound. The structure of the anion $[V^{III}(C_6Cl_5)_4]^-$ is depicted in Figure 1, and selected interatomic distances and

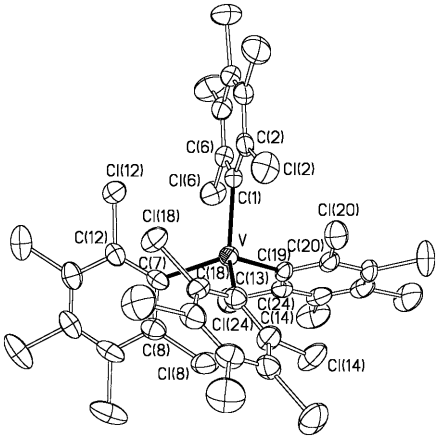

Figure 1. Thermal ellipsoid diagram (50% probability) of the anion of **1′**.

angles appear in Table 1. The vanadium centre is located in an approximately tetrahedral (*T*-4) environment with almost identical V−C bond lengths (mean value: 214.9(5) pm) and C−V−C angles ranging from 98.1(2)° to 117.6(2)°. Two of these angles are smaller than the ideal tetrahedral value (109.5°), while the remaining four are larger, thus resulting in a slight elongation of the tetrahedron. These angular distortions can reasonably be ascribed to the highly anisotropic character of the C_6Cl_5 rings, a feature noticed earlier not only in related organometallic species,[14] but also in simple main-group ER_4 derivatives with various polyatomic, monodentate R substituents.[15] The small value of the *T*-4 shape measure[16] obtained for **1′** ($S(T\text{-}4)$ = 0.805[17]) denotes that the angular distortions around the vanadium centre are of minor importance. It is also interesting to note that the overall geometry of the $[V^{III}(C_6Cl_5)_4]^-$ anion (d^2) is closely related to those found in the isoleptic species $[Ti^{III}(C_6Cl_5)_4]^-$ (d^1)[18] and $[Ti^{IV}(C_6Cl_5)_4]$ (d^0),[14] regardless of their different electron configurations. The local geometry around the V centre in **1′** is also similar to that found in the neutral species $[V^{IV}(mes)_4]$ (d^1):[19] the C−V−C angles in this species take values between 96.4(3)° and 117.8(3)° and the V−C distances are slightly shorter (207.1(6)–209.5(7) pm) than those found in **1′**, as would be expected with an increase in the oxidation state of the metal centre. All the C_6Cl_5 rings in the

Table 1. Selected bond lengths (pm) and angles (°) and their estimated standard deviations for the anion of **1′**.

Bond lengths			
V–C(1)	214.4(5)	C(2)–Cl(2)	174.6(6)
V–C(7)	215.8(5)	C(6)–Cl(6)	174.3(6)
V–C(13)	215.2(5)	C(7)–C(8)	138.7(7)
V–C(19)	214.2(5)	C(7)–C(12)	139.6(7)
V···Cl(2)	364.6(2)	C(8)–Cl(8)	173.4(6)
V···Cl(6)	311.6(2)	C(12)–Cl(12)	174.4(6)
V···Cl(8)	311.5(2)	C(13)–C(14)	139.3(7)
V···Cl(12)	366.3(2)	C(13)–C(18)	139.2(7)
V···Cl(14)	366.3(2)	C(14)–Cl(14)	174.8(6)
V···Cl(18)	313.6(2)	C(18)–Cl(18)	174.2(6)
V···Cl(20)	304.9(2)	C(19)–C(20)	138.0(7)
V···Cl(24)	368.3(2)	C(19)–C(24)	138.9(7)
C(1)–C(2)	139.2(7)	C(20)–Cl(20)	174.5(6)
C(1)–C(6)	138.7(7)	C(24)–Cl(24)	174.5(6)
Bond angles			
C(1)–V–C(7)	112.1(2)	C(8)–C(7)–C(12)	114.4(5)
C(1)–V–C(13)	117.6(2)	C(7)–C(8)–Cl(8)	117.1(5)
C(1)–V–C(19)	101.1(2)	C(7)–C(12)–Cl(12)	119.7(4)
C(7)–V–C(13)	98.1(2)	V–C(13)–C(14)	130.7(4)
C(7)–V–C(19)	116.1(2)	V–C(13)–C(18)	115.6(4)
C(13)–V–C(19)	112.6(2)	C(14)–C(13)–C(18)	113.5(5)
V–C(1)–C(2)	130.6(4)	C(13)–C(14)–Cl(14)	119.7(4)
V–C(1)–C(6)	115.2(4)	C(13)–C(18)–Cl(18)	116.9(4)
C(2)–C(1)–C(6)	114.2(5)	V–C(19)–C(20)	113.8(4)
C(1)–C(2)–Cl(2)	119.2(4)	V–C(19)–C(24)	132.0(4)
C(1)–C(6)–Cl(6)	117.0(4)	C(20)–C(19)–C(24)	114.2(5)
V–C(7)–C(8)	114.8(4)	C(19)–C(20)–Cl(20)	116.5(4)
V–C(7)–C(12)	130.4(4)	C(19)–C(24)–Cl(24)	119.5(4)

$[V^{III}(C_6Cl_5)_4]^-$ anion show marked swings about the *ipso*-C atom, as evidenced by the two significantly different V–C^{ipso}–C^{ortho} angles within each ring: for example, 130.6(4)° versus 115.2(2)° for the C(1)–C(6) ring. As a result, two clearly distinct V···Cl^{ortho} distances are also observed (311.6 vs 364.5 pm for the same ring as before, for example). We suggest that this swing does not per se necessarily imply any bonding interaction between the metal centre and the nearest *ortho*-Cl atom. Claims for the existence of such secondary bonding interactions, which have been documented in the chemistry of Cr^{III} (d^3),[20] Rh^{III} (d^6)[21] and Pt^{IV}(d^6),[22] should require some additional supporting evidence, such as 1) sufficiently short *ortho*-Cl···M distances, and 2) major angular distortions in the metal coordination environment, suggesting a higher coordination index as more appropriate. Since the *ortho*-Cl···V distances in **1′** are too long to be considered to arise from bonding interactions and, moreover, the geometry around the metal centre is satisfactorily described as a slightly elongated *T*-4 (cf. the *S*(*T*-4) value), the existence of *ortho*-Cl···V secondary bonding interactions in the homoleptic species $[V^{III}(C_6Cl_5)_4]^-$ can be ruled out. Moderate swings in the C_6Cl_5 rings had already been observed both in titanium and in main group nearly *T*-4 $[M(C_6Cl_5)_4]^{q-}$ compounds ($q=0$, M = Ti, Sn; $q=1$, M = Ti, Tl), and this feature was attributed to steric problems in the tetrahedral arrangement of these bulky ligands around the metal centre.[14]

The $[V^{III}(C_6Cl_5)_4]^-$ anion is remarkably stable, not being affected by the action of air or moisture. The V–C_6Cl_5 bonds do not undergo solvolytic processes in the presence of *i*PrOH or water. Complex **1** was treated with an equimolar amount of $[VCl_3(thf)_3]$ in thf at reflux, but no ligand exchange was observed to occur, at least over 10 h. No coordination of small molecules such as CO or NO to the $[V^{III}(C_6Cl_5)_4]^-$ anion was detected at room temperature and 1 bar pressure: no IR absorptions assignable to coordinated CO or NO could be observed, and starting product was recovered from the reaction media. The halide anions Cl^- or Br^- did not coordinate either. This failure to expand the coordination number of the vanadium centre in the $[V^{III}(C_6Cl_5)_4]^-$ anion is in keeping with the absence of any detectable *ortho*-Cl···V interaction in the molecular structure of **1′** (vide supra).

EPR spectra of the $[V^{III}(R_{Cl})_4]^-$ salts: As far as we know, EPR data currently available for the non-Kramers paramagnetic V^{III} entity (d^2, $S=1$) are extremely scarce. This paucity might well have been conditioned by the widespread belief that V^{III} is an "EPR-silent" system. In fact, the only reliable data of which we are aware have been obtained for V^{III} occupying high-symmetry sites in host lattices, such as cuboidal sites in highly ionic solids (e.g., CaF_2/V^{III}, $g=1.933$ and CdF_2/V^{III}, $g=1.937$)[23] or tetrahedral sites in ZnS-like semiconductors (V^{III}, $g=1.92$–1.99).[24] Only recently has it been possible to obtain EPR spectra of the six-coordinate species $[V(acac)_3]$, $[VX_3(thf)_3]$ (X = Cl, Br) and $[V(OH_2)_6]^{3+}$ by use of high-frequency techniques.[25,26]

Quite unexpectedly, well-defined X- and Q-band EPR spectra were obtained for powder samples of **1**–**3**. The room-temperature X-band spectra are similar for all three compounds (Figure 2), with four dominant features at magnetic field values lower than 1 T and no further signals detected up to 1.5 T (the upper limit of our spectrometer). The corresponding room-temperature Q-band spectra obtained from powder samples of **1**–**3** are to be found in the Supporting Information. The signal at $g\approx2$ observed in some of these measurements can be assigned to small amounts of oxidised V^{IV} species (see below).

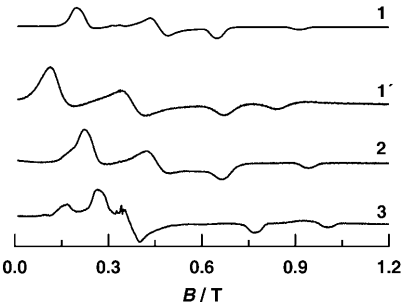

Figure 2. Room-temperature X-band EPR spectra of polycrystalline samples of **1**, **1′**, **2** and **3**.

In order to analyse the EPR spectra of **1**–**3**, we will assume slightly elongated *T*-4 structures for the complex anions $[V^{III}(R_{Cl})_4]^-$, as is actually found in **1′**. The stepwise splitting suffered by the ^3F ground term of the free V^{III} ion (spherical symmetry) when subjected to ligand fields of decreasing symmetry $T_d > D_{2d} > C_{2v}$ is given in Figure 3. The spin-Hamiltonian parameter properly describing the magnetic behaviour of V^{III} in the last two site symmetries will necessarily include a term accounting for the zero-field splitting (ZFS) contribution. In our particular case, the spin Hamiltonian, shown in Equation (1), was used:[27]

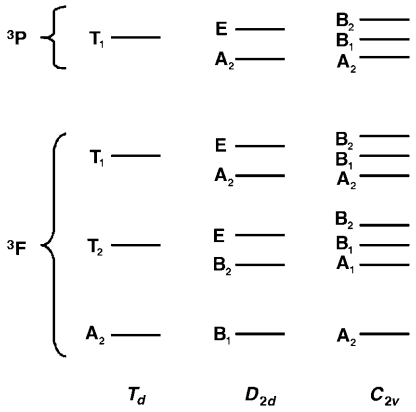

Figure 3. Electronic triplet spin states for the V^{III} ion under local fields of decreasing symmetry: $T_d > D_{2d} > C_{2v}$.

$$H = g\mu_B \vec{B} \cdot \vec{S} + D[S_Z^2 - {}^1/_3 S(S+1)] + E(S_X^2 - S_Y^2) \quad (1)$$

in which (*X*, *Y*, *Z*) are the principal axes of the ZFS tensor $\tilde{\boldsymbol{D}}$ and all other terms and components are according to standard notation. No anisotropy of the $\tilde{\boldsymbol{g}}$ tensor has been considered. Only a small anisotropic contribution, if any, would be expected for a ground term deriving from a $^3A_2$ one. Moreover, no clear evidence for $\tilde{\boldsymbol{g}}$ anisotropy could be observed in the experimental spectra. The omission of any hyperfine-contribution term in Equation (1) is justified because of the absence of well-resolved hyperfine structure in the experimentally measured spectra. An estimate of the spin-Hamiltonian parameters describing these V^{III} entities could be made by iterative comparison of EPR spectra calculated by exact diagonalisation of Equation (1) with the experimentally obtained ones. Satisfactory agreements were achieved with the spin-Hamiltonian parameters given in Table 2, as illustrated for complex **1** in Figure 4 (X-band). It is worth noting that the same set of parameters allows both the X- and the Q-band spectra to be reproduced (Figures S1–S6 in the Supporting Information). Noticeable differences between the experimentally measured EPR spectra of **1** and **1′** were found (Figure 2); this can be ascribed not so much to important structural changes in the common $[V^{III}(C_6Cl_5)_4]^-$ anions but rather to lattice effects caused by the different cations present in each case ($[Li(thf)_4]^+$ vs $[NBu_4]^+$).

Table 2. Spin-Hamiltonian parameters for the different salts of the homoleptic organovanadium(III) anions $[VR_4]^-$.

Compound	*g*	*D* [GHz]	*E* [GHz]	$\eta = E/D$
$[Li(thf)_4][V(C_6Cl_5)_4]$ (**1**)	1.96	15.38	1.32	0.086
$[NBu_4][V(C_6Cl_5)_4]$ (**1′**)	1.98	13.59	2.10	0.155
$[Li(thf)_4][V(tcp)_4]$ (**2**)	1.95	15.93	1.46	0.092
$[Li(thf)_4][V(dcp)_4]$ (**3**)	1.96	17.69	2.75	0.155
$[Li(thf)_4][V(mes)_4]$	1.95	15.02	0.30	0.020

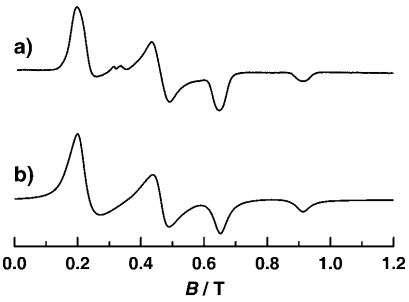

Figure 4. Room-temperature X-band EPR spectra of a polycrystalline sample of **1**: a) experimentally measured; b) calculated with the spin-Hamiltonian parameters given in Table 2.

As shown in Table 2, the values of the ZFS *D* parameter obtained for compounds **1**–**3** (*D* ca. 15 GHz) are of the same order of magnitude as the exciting frequency used in our EPR experiments (ca. 9.5 GHz in X band, ca. 35 GHz in Q band), allowing us to observe defined EPR spectra for compounds **1**–**3** and **1′**. The fact that *D* and *hν* are comparable in magnitude in these systems should be intimately related to the particular distribution of energy levels obtained for the slightly distorted *T*-4 geometry assumed for all the $[V^{III}(R_{Cl})_4]^-$ anions (cf. the much higher *D* values obtained for the *OC*-6 species $[V(acac)_3]$, $[VX_3(thf)_3]$ and $[V(OH_2)_6]^{3+}$ mentioned above, which could be detected only under high-field and high-frequency conditions: *hν* up to 700 GHz).[26] In order to check the validity of this conclusion, we measured the EPR spectrum of a related tetrasubstituted homoleptic vanadium(III) species for which a similar *T*-4 structure could also be reasonably assumed: the salt $[Li(thf)_4][V^{III}(mes)_4]$.[3] The room-temperature EPR spectrum of a polycrystalline sample of $[Li(thf)_4][V^{III}(mes)_4]$ (Figure 5a) was indeed found to be similar to those just discussed for **1**–**3** (Figure 2). The spin-Hamiltonian parameters derived from analysis of this spectrum by use of Equation (1) are given in Table 2 (simulated spectrum in Figure 5b), and also show remarkable similarities to those corresponding to the polychlorophenyl derivatives **1**–**3**. A particularly small value of $\eta = 0.020$ denotes the lowest degree of orthorhombicity within the series.

The electronic absorption spectra of **1** and $[Li(thf)_4][V^{III}(mes)_4]$[28] were also measured (Figure 6), with the goal of obtaining more information about the actual energy-level

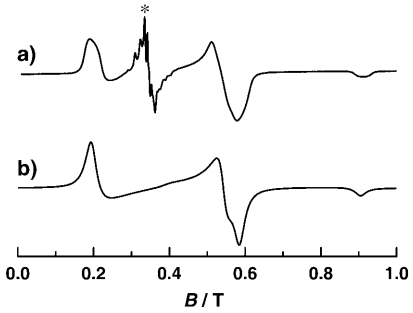

Figure 5. Room-temperature X-band EPR spectrum of a polycrystalline sample of $[Li(thf)_4][V^{III}(mes)_4]$: a) experimentally measured; b) calculated with the spin-Hamiltonian parameters given in Table 2. The signal marked *, showing hyperfine structure, is attributed to a comparatively small quantity of $[V^{IV}(mes)_4]$.

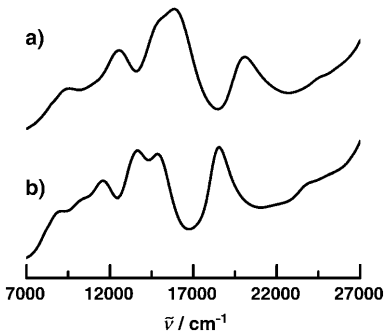

Figure 6. Room-temperature electronic absorption spectra of **1** in CH_2ClCH_2Cl (a) and of $[Li(thf)_4][V(mes)_4]$ in thf (b).

distribution for the $[V^{III}R_4]^-$ species. These spectra can be explained by use of a standard ligand field potential with the absorption band assignment shown in Table 3. The two, in principle, equally valid assignments for the $^3A_2(^3A_2)\rightarrow{}^3B_1(^3T_2)$ and $^3A_2(^3A_2)\rightarrow{}^3A_2(^3T_1)$ transitions are also given in Table 3. The values of the Racah *B* and crystal-field parameters deduced from these assignments are shown in Table 4. A reasonably good agreement is observed between the spin-Hamiltonian parameters obtained for the mesityl and pentachlorophenyl derivatives from EPR measurements and those derived from electronic absorption spectra (see Supporting Information); this can be taken as evidence of the suitability of our approach for analysis of these systems. Moreover, the fact that $Dt/Dq>0$ in the two referred compounds, as to be expected for an elongated distortion,[29] lends further support to our initial structural proposal for all the $[V^{III}R_4]^-$ species under study. These results underline the usefulness of EPR spectroscopy as a valuable structural tool in the chemistry of open-shell organometallic compounds ($S\geq{}^1/_2$). It also becomes clear that the widespread idea of V^{III} being an "EPR-silent" entity, under conventional measuring conditions of field and frequency, should be abandoned.

Table 3. Band positions (cm^{-1}) in the electronic absorption spectra of the $[Li(thf)_4][VR_4]$ derivatives (R = C_6Cl_5, mes) with their corresponding transition assignments.[a]

Transition[b] $^2A_2(^3A_2)\rightarrow$ (I)	(II)	$[Li(thf)_4][V^{III}R_4]$ R = C_6Cl_5	R = mes
	$^3A_1(^3T_2)$	9400	9139
	$^3B_2(^3T_2)$	12550	11610
$^3A_2(^3T_1)$	$^3B_1(^3T_2)$	14970	13680
$^3B_1(^3T_2)$	$^3A_2(^3T_1)$	15925	14840
	$^3B_1(^3T_1)$	20070	18550
	$^3B_2(^3T_1)$	24525	23460

[a] Assignments made with the aid of the following effective crystal-field potential: $H_{CF}=h_{2,0}\tilde{C}_{2,0}+h_{2,2}(\tilde{C}_{2,+2}+\tilde{C}_{2,-2})+h_{4,0}\tilde{C}_{4,0}+h_{4,2}(\tilde{C}_{4,+2}+\tilde{C}_{4,-2})+h_{4,4}(\tilde{C}_{4,+4}+\tilde{C}_{4,-4})$, where $\tilde{C}_{k,q}$ is the sum extended to all the d electrons of the monoelectronic Racah operator $\tilde{C}(\theta,\phi)$ and the $h_{k,q}$ parameters account for the interaction strength; for further details see Supporting Information. [b] Energy levels labelled as in Figure 3.

Table 4. Values (cm^{-1}) of the Racah *B* and crystal-field parameters[a] best fitting the electronic absorption spectra of $[Li(thf)_4][VR_4]$ (R = C_6Cl_5, mes).

	$[Li(thf)_4][V^{III}(C_6Cl_5)_4]$ (I)	(II)	$[Li(thf)_4][V^{III}(mes)_4]$ (I)	(II)
B[b]	720	707	680	650
Dq[c]	−1290	−1290	−1215	−1200
Dt[c]	−355	−350	−300	−300
$h_{2,0}$	9870	7760	10110	7415
$h_{2,2}$	−3750	−2944	−2170	−1220
$h_{4,4}$	−5510	−6227	−5420	−6350

[a] Parameters named according to Table 3, footnote [a]. [b] For the free V^{3+} ion, $B_0=860\ cm^{-1}$. [c] The Dq and Dt parameters are introduced in a conventional way and are related to $h_{4,0}$ and $h_{4,4}$ by the following expressions: $h_{4,0}=21(Dq+Dt)$, $h_{4,0}=-105(Dq-Dt)/\sqrt{70}$; in T_d symmetry, $Dt=0$ and Dq is the standard crystal-field splitting parameter.

Synthesis and characterisation of the $[V^{IV}(R_{Cl})_4]$ compounds: In our experience, the C_6Cl_5 group has been shown to be a ligand especially suitable for stabilising homoleptic compounds with the metal in different oxidation states. Tetrasubstituted homoleptic compounds with different geometries have thus been prepared for the following series of metal centres: Ti^{IV}/Ti^{III},[14] $Cr^{IV}/Cr^{III}/Cr^{II}$,[20a] Rh^{III}/Rh^{II}[21] and $Pt^{IV}/Pt^{III}/Pt^{II}$.[30] It therefore seemed advisable to study the redox behaviour of compounds **1**–**3** by electrochemical methods. The room-temperature cyclic voltammogram (CV) of solutions of $[V^{III}(C_6Cl_5)_4]^-$ in CH_2Cl_2, scanned at $100\ mV\,s^{-1}$ from −1.6 to 1.6 V and then back to −1.6 V, shows a single oxidation wave ($(E_p)_{ox}=0.88$ V), which is recovered in the returning scan ($(E_p)_{red}=0.79$ V), corresponding to an electrochemically reversible semisystem ($E_{1/2}=0.83$ V, $\Delta E_p=0.09$ V, $i_{pa}/i_{pc}=0.99$). Solutions of **2** and **3** in CH_2Cl_2 showed qualitatively similar behaviour. However, the mean potential of the electrochemically reversible semisystem was observed to decrease distinctly in the following order: **1** > **2** > **3** (Table 5). It becomes apparent that the degree of chlorination of the R_{Cl} group has a great effect on the stability of the V^{IV} species relative to the V^{III} one. A decrease in the degree of chlorination of R_{Cl} should enhance its donor ability, thereby favouring the stabilisation of the oxidised (and more acidic) species. This effect is even more pronounced if the highly electronegative Cl substituents on

Table 5. Electrochemical data (cyclic voltammetry) obtained for the polychlorophenylvanadate(III) compounds $[Li(thf)_4][V(R_{Cl})_4]$ (**1–3**).[a]

Compound	R_{Cl}	$(E_p)_{ox}$ [V]	$(E_p)_{red}$ [V]	ΔE_p [V]	$E_{1/2}$ [V]	i_{pa}/i_{pc}
1	C_6Cl_5	0.88	0.79	0.09	0.83	0.99
2	tcp	0.47	0.37	0.10	0.42	1.05
3	dcp	0.30	0.21	0.09	0.25	1.10

[a] In CH_2Cl_2; scan rate = 100 mV s^{-1}.

the phenyl ring are replaced by positively inductive methyl groups; thus, in the $[V^{IV}(mes)_4]/[V^{III}(mes)_4]^-$ semisystem, the neutral V^{IV} species is known to be the more stable.[31]

In view of these results we sought to prepare the oxidised species involved in the redox systems by chemical methods. Indeed, the homoleptic neutral compounds $[V^{IV}(R_{Cl})_4]$ ($R_{Cl} = C_6Cl_5$ (**4**), tcp (**5**), dcp (**6**)) were obtained in reasonable yields by treatment of the corresponding vanadium(III) precursor with the appropriate oxidising agent (Scheme 2).[32] Compounds **4–6** were isolated as blue solids

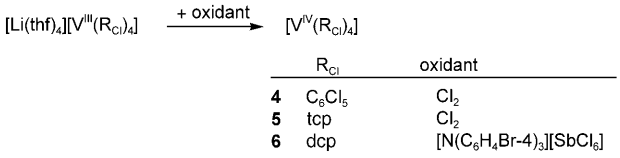

Scheme 2. Production of the homoleptic neutral compounds arylvanadium(IV) compounds **4–6**.

of rather limited thermal stability. Complex **4** dissolved in thf undergoes spontaneous reduction to the anionic parent species $[V^{III}(C_6Cl_5)_4]^-$. Special caution must be taken with compound **6**, because it has been observed to explode violently by percussion even at low temperatures. This instability notwithstanding, the characterisation of compounds **4–6** could be carried out by analytical and spectroscopic methods.

The mass spectra (FAB^-) of **4** and **5** are similar to those of their corresponding precursors **1** and **2**. However, neither positive nor negative ions could be detected in the mass spectra of **6** run under different ionisation conditions and with use of various types of matrices. In the IR spectrum of **4**, the band attributable to the X-sensitive vibration of the C_6Cl_5 group[12] appears as a strong absorption at a significantly higher wavenumber (842 cm^{-1}) than observed in the vanadium(III) species **1** or **1′** (ca. 829 cm^{-1}).

Cyclic voltammetry experiments on **4–6** gave results similar to those observed for **1–3** (Table 5), thus confirming the electrochemical relationship between the two triads of compounds.

Although no unequivocal structural information for compounds **4–6** is yet available, we suggest elongated *T*-4 structures, as have been established for the isoelectronic $[Ti^{III}(C_6Cl_5)_4]^-$ species,[18] as well as for the related compound $[V(mes)_4]$.[19] The EPR spectroscopic data of compounds **4–6**, which can be satisfactorily explained by this structural proposal (see below) are in keeping with this assumption.

EPR spectra of the $[V^{IV}(R_{Cl})_4]$ compounds: The EPR spectra of the neutral compounds **4–6**, containing the Kramers paramagnetic V^{IV} entity (d^1, $S = 1/2$) were measured under various conditions. Similar spectra were observed in all three cases, so only the results obtained for $[V^{IV}(C_6Cl_5)_4]$ (**4**) are described in detail. The room-temperature EPR spectrum of a polycrystalline sample of **4** (Figure 7a) shows a broad signal centred at $g \approx 2$ with a poorly resolved hyper-

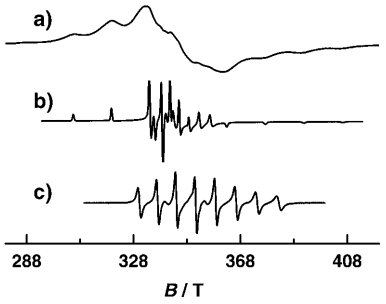

Figure 7. X-band EPR spectra of **4**: a) polycrystalline sample measured at room temperature; b) solution in CH_2Cl_2/CH_2ClCH_2Cl (1:1) measured at 77.3 K; c) solution in CH_2Cl_2/CH_2ClCH_2Cl (1:1) measured at room temperature.

fine structure due to the ^{51}V nucleus ($I = 7/2$, 99.75 % natural abundance).[33] Better resolution is achieved by working on chilled (Figure 7b) or fluid (Figure 7c) solutions of **4** in CH_2Cl_2/CH_2ClCH_2Cl (1:1) mixtures. If orbitally nondegenerate electronic ground states are assumed for compounds **4–6**, their magnetic properties should, in general, be given by the spin Hamiltonian shown in Equation (2):

$$H = \mu_B \vec{B} \cdot \tilde{\boldsymbol{g}} \cdot \vec{S} + \vec{I} \cdot \tilde{\boldsymbol{A}} \cdot \vec{S} \quad (2)$$

in which $\tilde{\boldsymbol{g}}$ and $\tilde{\boldsymbol{A}}$ represent the gyromagnetic and hyperfine coupling tensors, respectively. In fluid solution, the molecular tumbling should smear out the anisotropic contributions of the $\tilde{\boldsymbol{g}}$ and $\tilde{\boldsymbol{A}}$ tensors and so the spectra obtained under these conditions should be described by an isotropic spin Hamiltonian shown in Equation (3):

$$H = \mu_B g \vec{B} \cdot \vec{S} + a \vec{I} \cdot \vec{S} \quad (3)$$

in which the scalar *g* factor and the hyperfine coupling constant *a* are related to the preceding tensors by: $g = \mathrm{tr}(\tilde{\boldsymbol{g}})/3$ and $a = \mathrm{tr}(\tilde{\boldsymbol{A}})/3$. A single set of *g* and *a* values was obtained from the EPR spectra of the three $[V^{IV}(R_{Cl})_4]$ compounds (**4–6**) in fluid solution: $g = 1.965(5)$, $a = 185(1)$ MHz.

The EPR spectrum of **4** in frozen solution (Figure 7b) denotes that the hyperfine tensor $\tilde{\boldsymbol{A}}$ is markedly anisotropic, with one of the principal values, namely A_z, being dominant. This is in keeping with the elongated *T*-4 structure (approximately C_{2v}) suggested for compounds **4–6** (see above). In this particular case, the outer features are determined by the corresponding principal values of the $\tilde{\boldsymbol{g}}$ tensor and the hyperfine coupling constant (g_z and A_z); these values are, in practice, independent of the other components. This has allowed us to make estimates of the A_z and g_z values, which have been found to be virtually identical for all three compounds **4–6**: $g_z = 1.925(5)$, $A_z = 385(2)$ MHz. Moreover, as $g_z < g < g_e$ ($g_e = 2.0023$ for the free electron), it can be concluded that the ground-state orbitals for compounds **4–6** are each $a_2(xy)$—as to be expected for elongated *T*-4 coordination environments.[34] The electronic energy levels for V^{IV} in such a local symmetry are shown in Figure 8. The admixture

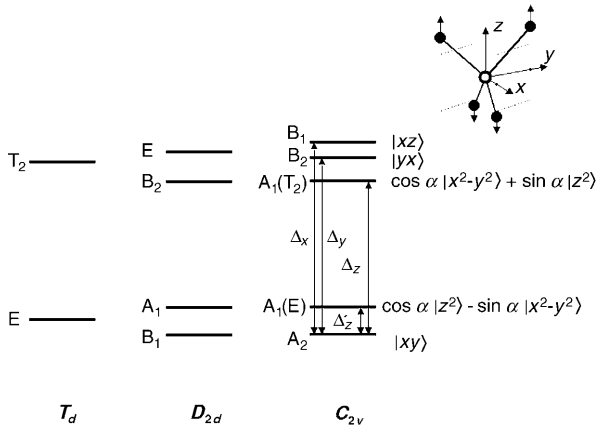

Figure 8. Electronic energy levels corresponding to the V^{IV} ion under local fields of decreasing symmetry: $T_d > D_{2d} > C_{2v}$. The inset shows the coordinate axes chosen for the orbital labelling (see Supporting Information for details).

of the $|z^2>$ and $|x^2-y^2>$ levels, which is given by the value of α, is a consequence of some degree of orthorhombic distortion. If these low-symmetry contributions are considered only up to a first order referring to the tetrahedral and tetragonal energy splittings, such an admixture can be neglected ($\alpha = 0$). In this case, and according to conventional theory,[27] the principal values of the $\tilde{\boldsymbol{g}}$ tensor are given by Equation (4):

$$g_x = g_e - \frac{2\lambda}{\Delta_x}\ ,\quad g_y = g_e - \frac{2\lambda}{\Delta_y}\ ,\quad g_z = g_e - \frac{8\lambda}{\Delta_z} \tag{4}$$

and those of the hyperfine $\tilde{\boldsymbol{A}}$ tensor by Equations (5x–z):

$$A_x = -P\left\{\kappa + (g_e - g_x) - \frac{3}{14}(g_e - g_y) - \frac{2}{7}\right\} \tag{5x}$$

$$A_y = -P\left\{\kappa + (g_e - g_y) - \frac{3}{14}(g_e - g_x) - \frac{2}{7}\right\} \tag{5y}$$

$$A_z = -P\left\{\kappa + (g_e - g_z) + \frac{3}{14}(g_e - g_x) + \frac{3}{14}(g_e - g_y) + \frac{4}{7}\right\} \tag{5z}$$

where *P* is defined according to Equation (6):

$$P = g_e g_n \mu_B \mu_n \langle r^{-3} \rangle \tag{6}$$

and κ is related to the spin density in the metal nucleus, χ, by Equation (7):

$$\chi = -\frac{2}{3}\kappa \langle r^{-3} \rangle \tag{7}$$

As the only data available for compounds **4–6** are those corresponding to the isotropic contributions of the $\tilde{\boldsymbol{g}}$ and $\tilde{\boldsymbol{A}}$ tensors, *g* and *a*, together with their axial components, g_z and A_z, it is more convenient to use the following expressions [Eqs. (8)–(10)], which are straightforwardly obtained from those given above:

$$a = -P\{\kappa + (g_e - g)\} \tag{8}$$

$$A_z = -P\left\{\kappa + \frac{11}{14}(g_e - g_z) + \frac{9}{14}(g_e - g) + \frac{4}{7}\right\} \tag{9}$$

$$A_z - a = -P\left\{\frac{11}{14}(g_e - g_z) - \frac{5}{14}(g_e - g) + \frac{4}{7}\right\} \tag{10}$$

By introducing the experimentally determined values of *g*, g_z, *a* and A_z (see above) in these equations, the following values are obtained: $|P| = 323(4)$ MHz, $|\kappa| = 0.54(1)$, $\langle r^{-3} \rangle = 2.32(3)$ a.u.

The electronic absorption spectrum of a solution of **4** in CH_2ClCH_2Cl (Figure 9) shows three bands at 14950, 16680 and 21400 cm^{-1}, the first two being strongly overlapped. These absorptions correspond to the Δ_i ($i = x, y, z$) transitions in Equation (4). Although no unequivocal assignment can, in principle, be made, we attribute the experimentally observed absorption bands in order of increasing frequency

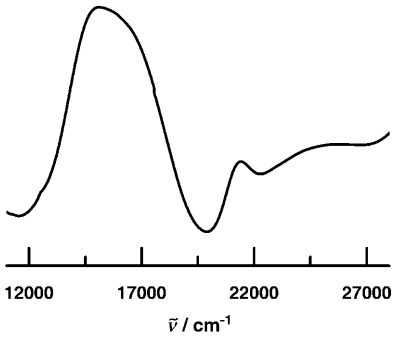

Figure 9. Room-temperature electronic absorption spectrum of **4** in CH_2ClCH_2Cl.

to the transitions from the $a_2(xy)$ ground state to the $a_1(x^2-y^2)$, $b_2(yz)$ and $b_1(xz)$ excited states, respectively (Figure 8). This assignment has been made by taking account of the fact that the EPR data strongly suggest a practically axial $\tilde{g}$ tensor. From Equation (4) it would be possible to estimate the principal values of the $\tilde{g}$ tensor should the value of the spin-orbit coupling constant (λ) be known. For the V^{4+} free ion, $\lambda_0 = 250\ cm^{-1}$,[35] but the actual value of λ in any real chemical species is usually reduced due to covalency effects. In particular, taking $\lambda = 198\ cm^{-1}$ (ca. 80% of λ_0), we obtain:

$$g_x = 1.976,\ g_y = 1.978,\ g_z = 1.928,\ g = 1.961,$$

which is in good agreement with the experimentally obtained EPR data. It is worth noting that the difference $g_y - g_x = 0.002$ lies within the experimental error involved in determining these parameters and denotes a small degree of orthorhombicity in the systems, as pointed out above.

The relevant EPR parameters obtained for compounds **4**–**6** are presented in Table 6, together with those corresponding to other known $[VR_4]$ species in which R is a singly charged, monodentate ligand.[36–39] The value of the $\langle r^{-3}\rangle/\langle r^{-3}\rangle_0$ quotient, where $\langle r^{-3}\rangle_0 = 3.67$ a.u., as calculated for free V^{IV} from the Clementi and Roetti wave functions,[40] seems of particular importance to us, as it is related to the covalent character of the V^{IV}–R bond. The $\langle r^{-3}\rangle/\langle r^{-3}\rangle_0$ values for the different $[VR_4]$ species shown in Table 6 follow the sequence $C_6Cl_5 \approx NEt_2 > OCMe_3 > mes > SCMe_3$, and so it can be concluded that the V^{IV}–C_6Cl_5 bond is in the upper range of ionic character for such homoleptic species. The behaviour of the perchlorinated and partially chlorinated phenyl groups is, however, indistinguishable in these d^1 ($S = {}^1/_2$) systems **4**–**6**, from the EPR point of view.

Table 6. Spin-Hamiltonian parameters for neutral, homoleptic $[V^{IV}R_4]$ species derived from the analysis of available data under a local C_{2v} symmetry.

Compound	g_z	g_{iso}	A_z [MHz]	a_{iso} [MHz]	$\langle r^{-3}\rangle/\langle r^{-3}\rangle_0$	Ref.
$[V(C_6Cl_5)_4]$ (**4**)[a]	1.925	1.965	385	185	0.63	–[b]
$[V(NEt_2)_4]$	1.949	1.961	369	175	0.63	[36]
$[V(OCMe_3)_4]$	1.940	1.969	374	190	0.59	[37]
$[V(mes)_4]$	1.925	1.968	370	190	0.56	[38]
$[V(SCMe_3)_4]$	1.961	1.970	297	151	0.48	[39]

[a] The same values are obtained for compounds **5** and **6**. [b] This work.

Synthesis and characterisation of $[NBu_4]_2[V^{III}(C_6F_5)_5]$ (7): In contrast to the behaviour observed with the polychlorophenyl ligands R_{Cl}, treatment of $[VCl_3(thf)_3]$ with LiC_6F_5 at −78 °C, followed by the addition of NBu_4Br at −30 °C, resulted in the formation of $[NBu_4]_2[V^{III}(C_6F_5)_5]$ (**7**), which was isolated as an air- and moisture-sensitive, light green solid (Scheme 1). To the best of our knowledge, the $[VR_5]^{2-}$ stoichiometry is unprecedented in organometallic chemistry. Compound **7** must be handled with great caution and kept at low temperature (−30 °C) because it is prone to explode by percussion and easily undergoes thermal decomposition. Nonetheless, analytical and spectroscopic data could be obtained for **7** and its crystal structure was established by using X-ray diffraction methods.

In the mass spectra (FAB^-) of **7**, the peak with the highest mass (m/z 905) can be assigned to the $[V(C_6F_5)_5F]^-$ ion. The origin of the extra fluoro ligand is uncertain. No sign of the uptake of any further ligand is observed in any of the lower-mass peaks, the formulas of which conform simply to the sequential loss of C_6F_5 groups: $[V(C_6F_5)_n]^-$ ($n = 4, 3, 2$).

The IR spectrum of **7** contains a broad and weak absorption at 800 cm^{-1}, which can be assigned to the X-sensitive vibration mode of the C_6F_5 group.[12] Similar features were observed in the isoleptic $[M(C_6F_5)_5]^{2-}$ species of the neighbouring elements Ti and Cr, for which trigonal bipyramidal (*TBPY*-5)[41] and square pyramidal (*SPY*-5)[42] structures, respectively, were established. These related species both gave single, sharp absorptions at approximately 946 cm^{-1} due to the ν(C–F) vibration modes, while two very strong bands at 937 and 949 cm^{-1} were observed in the IR spectrum of **7**. The origin of this different vibrational behaviour is still not clear.

Crystals of **7** are composed of discrete $[NBu_4]^+$ and $[V^{III}(C_6F_5)_5]^{2-}$ ions (in 2:1 ratio) as determined by using single-crystal X-ray diffraction analysis. A selection of relevant interatomic distances and interbond angles is given in Table 7. The structure of the vanadium(III) complex anion (Figure 10) can be described as slightly distorted *TBPY*-5, according to the continuous shape measure for this geometry: $S(TBPY\text{-}5) = 0.977$.[17] The mutual arrangement of the V–C_{ax} bonds departs only slightly from linearity (C(19)–V–C(25) 176.3(2)°). Axial C_6F_5 groups are observed to adopt a staggered conformation. The sum of the C_{eq}–V–C'_{eq} angles amounts to 359.89(2)°, denoting no pyramidalisation around the V centre. The failure of the equatorial C_6F_5 groups to adopt a helicoidal arrangement can be taken as the primary source of the pronounced Y-distortion: C_{eq}–V–C'_{eq} angles of approximately 126° are observed between disrotatory rings, while the angle between the two conrotatory rings is significantly more closed: C(1)–V–C(13) = 107.3(2)°. The V–C_{ax} bonds (221.7(5) and 219.3(5) pm) are significantly longer than the V–C_{eq} ones (213.6(5)–216.8(5) pm), according to the behaviour theoretically predicted for transition-metal (*TBPY*-5)-$[ML_5]$ species with d^n ($n < 5$) electron configuration.[43] The mean V^{III}–C bond length in **7** (217.2(5) pm) is slightly longer than that found in **1′** (214.9(5) pm). This difference can reasonably be ascribed to the different coordination numbers and global charges in the two anionic species compared ($[VR_5]^{2-}$ vs $[VR_4]^-$).

The overall geometry of the d^2 anion $[V^{III}(C_6F_5)_5]^{2-}$ is similar to, but more regular than, that found in the d^1 isoleptic species $[Ti^{III}(C_6F_5)_5]^{2-}$, for which not only a Y distortion but also an appreciable departure of the C_{ax}–V–C'_{ax} angle from linearity (164.6(2)°) have been observed, thus resulting in a totally reversed Berry distortion.[41] The more regular geometry of the V^{III} species **7** can be related to the orbitally non-

Table 7. Selected bond lengths (pm) and angles (°) and their estimated standard deviations for the anion of **7**.

Bond lengths			
V–C(1)	214.5(5)	C(13)–C(14)	139.7(7)
V–C(7)	216.8(5)	C(13)–C(18)	138.4(6)
V–C(13)	213.6(5)	C(14)–F(14)	135.7(5)
V–C(19)	219.3(5)	C(18)–F(18)	136.3(5)
V–C(25)	221.7(5)	C(19)–C(20)	138.1(7)
C(1)–C(2)	137.5(6)	C(19)–C(24)	138.4(7)
C(1)–C(6)	136.3(6)	C(20)–F(20)	138.0(5)
C(2)–F(2)	135.9(5)	C(24)–F(24)	137.0(5)
C(6)–F(6)	136.8(5)	C(25)–C(26)	138.4(7)
C(7)–C(8)	137.7(7)	C(25)–C(30)	137.1(7)
C(7)–C(12)	139.0(7)	C(26)–F(26)	137.3(6)
C(8)–F(8)	136.9(5)	C(30)–F(30)	137.1(5)
C(12)–F(12)	135.4(5)		
Bond angles			
C(1)–V–C(7)	127.1(2)	C(8)–C(7)–C(12)	111.6(4)
C(1)–V–C(13)	107.3(2)	C(7)–C(8)–F(8)	120.0(4)
C(1)–V–C(19)	99.5(2)	C(7)–C(12)–F(12)	120.0(4)
C(1)–V–C(25)	82.1(2)	V–C(13)–C(14)	124.6(4)
C(7)–V–C(13)	125.4(2)	V–C(13)–C(18)	122.9(4)
C(7)–V–C(19)	89.3(2)	C(14)–C(13)–C(18)	112.4(5)
C(7)–V–C(25)	87.1(2)	C(13)–C(14)–F(14)	117.9(4)
C(13)–V–C(19)	84.5(2)	V–C(19)–C(20)	117.4(4)
C(13)–V–C(25)	98.2(2)	V–C(19)–C(24)	131.8(4)
C(19)–V–C(25)	176.3(2)	C(20)–C(19)–C(24)	110.7(5)
V–C(1)–C(2)	122.6(4)	C(19)–C(20)–F(20)	119.0(4)
V–C(1)–C(6)	123.9(3)	C(19)–C(24)–F(24)	119.3(4)
C(2)–C(1)–C(6)	113.0(4)	V–C(25)–C(26)	115.9(4)
C(1)–C(2)–F(2)	120.1(4)	V–C(25)–C(30)	131.2(4)
C(1)–C(6)–F(6)	119.6(4)	C(26)–C(25)–C(30)	112.6(5)
V–C(7)–C(8)	124.1(4)	C(25)–C(26)–F(26)	119.6(5)
V–C(7)–C(12)	124.2(4)	C(25)–C(30)–F(30)	120.6(4)

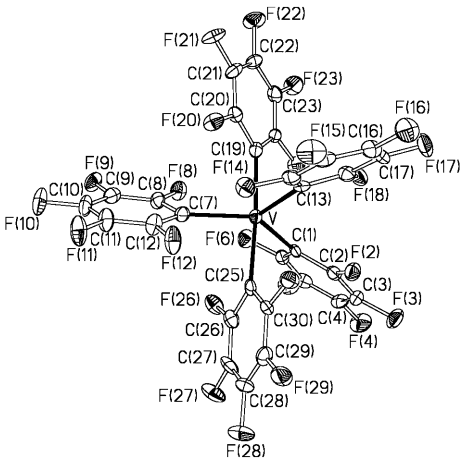

Figure 10. Thermal ellipsoid diagram (50% probability) of the anion of **7**.

degenerate $e''(xz,yz)^2$ electronic structure expected in an ideal *TBPY*-5 coordination environment, not violating the Jahn–Teller theorem.[44] The mean V^{III}–C bond length in **7** (217.2(5) pm) is slightly shorter than the mean Ti^{III}–C bond length (223.1(7) pm) found in its Ti^{III} homologue, according to the small contraction generally observed on going from Ti to V. It is also interesting to note that the d^3 species $[Cr^{III}(C_6F_5)_5]^{2-}$ has, in turn, a *SPY*-5 geometry with even more contracted M–C bonds (average Cr^{III}–C bond length: 214.7(2) pm).[42]

In contrast to the behaviour discussed above for the four-coordinate $[V(R_{Cl})_4]^-$ species **1**–**3**, no EPR spectrum was observed for **7** either in X or in Q band, most probably because the ZFS is much higher than the microwave frequency in this five-coordinate compound. Problems arising from inadequate relaxation times of the excited electron spin states cannot be excluded either. The electrochemical behaviour of compound **7** was studied by CV, but no defined electron-exchange process was observed between −1.6 and +1.6 V in CH_2Cl_2.

Conclusion

Important structural and spectroscopic differences have been found in homoleptic organovanadium(III) compounds containing σ-bound polyhalophenyl groups R. The spectroscopic and redox behaviour is also strongly dependent on the nature of R.

Polychlorophenyl groups, in which the *ortho* positions are invariably occupied by Cl atoms ($R_{Cl}=C_6Cl_5$, tcp, dcp) have been found to yield a series of electrochemically related $[V^{IV}(R_{Cl})_4]/[V^{III}(R_{Cl})_4]^-$ systems. The potentials of these V^{IV}/V^{III} redox couples depend on the electron-withdrawing character of the R_{Cl} group, which is directly related to the degree of chlorination of the phenyl ring. Defined EPR spectra have been obtained for all these homoleptic species (**1**–**6**). The fact that the non-Kramers (d^2, $S=1$) anions $[V^{III}(R_{Cl})_4]^-$ in **1**–**3** are not EPR-silent—as generally accepted for V^{III} compounds—is attributed to the particular distribution of energy levels originating from the slightly distorted *T*-4 geometry found in the 10-electron species $[NBu_4][V^{III}(C_6Cl_5)_4]$ (**1′**) by using X-ray diffraction methods. For the d^1 neutral compounds $[V^{IV}(R_{Cl})_4]$ (**4**–**6**), approximately *T*-4 structures can also be reasonably assumed (9-electron species).

With the less sterically demanding C_6F_5 group, a higher coordination number was achieved for V^{III} and so the five-coordinate, 11-electron compound $[NBu_4]_2[V^{III}(C_6F_5)_5]$ (**7**) was obtained, with a stoichiometry unprecedented in organovanadium chemistry. No EPR spectrum was observed for this non-Kramers (d^2, $S=1$) species, for which a *TBPY*-5 structure has been established (X-ray diffraction). The different coordination numbers expected for the adjacent oxidation states (most commonly 6 for V^{II} and 4 for V^{IV}) would justify the absence of any reversible electron-exchange process in the CV of **7**.

C_6F_5 and C_6Cl_5, reportedly possessing similarly electron-withdrawing characters,[45] show sharply different behaviour in their vanadium chemistry. In contrast, fairly homogeneous behaviour was observed within the series of R_{Cl} ligands essayed, for which differently electron-withdrawing characters depending on the degree of chlorination of the phenyl ring were to be expected. In view of these results, we con-

clude that the documented ability of the C_6Cl_5 group to enable the formation of homoleptic σ-organyl derivatives in different oxidation states for a given metal (M = Ti,[14] V, Cr,[20] Rh[21] and Pt[30]) relies more on the shielding effect exerted by the *ortho*-Cl substituents than on the group's electron-withdrawing properties. This would also explain the close relationship between the metal chemistries of the C_6Cl_5 and the mesityl ligands, given that similar van der Waals volumes are ascribed to the Cl and CH_3 substituents (0.0195 and 0.0222 nm^3, respectively).[46]

Experimental Section

General procedures and materials: All reactions and manipulations were carried out under purified argon by use of Schlenk techniques. Solvents were dried by standard methods and distilled prior to use. The vanadium complexes $[VCl_3(thf)_3]$[47] and $[Li(thf)_4][V(mes)_4]$[3] were prepared by literature methods. Ethereal solutions of the organolithium reagents Li(tcp) and Li(dcp) were prepared by low-temperature treatment of 1,3,5-trichloro-2-iodobenzene[48] or 1-bromo-2,6-dichlorobenzene (Acros Organics) with *n*BuLi by procedures similar to those described for the synthesis of LiC_6F_5[49] and LiC_6Cl_5.[50] The aminium salt $[N(C_6H_4Br\text{-}4)_3][SbCl_6]$ was purchased (Aldrich) and used as received. Solutions of chlorine were prepared by bubbling a stream of the dry gas through CCl_4 and were titrated by standard redox methods[51] before use. Electronic absorption spectra were measured in a Cary 500 spectrophotometer (Varian), in quartz sample holders. Elemental analyses were carried out with a Perkin–Elmer 2400-Series II microanalyzer. IR spectra (KBr discs) were recorded on a Perkin–Elmer Spectrum One spectrophotometer (4000–350 cm^{-1}). Mass spectra were recorded on a VG-Autospec spectrometer by standard Cs ion FAB (acceleration voltage: 35 kV). Electrochemical studies were carried out with an EG&G model 273 potentiostat in conjunction with a three-electrode cell, in which the working electrode was a platinum disc, the auxiliary electrode a platinum wire and the reference an aqueous saturated calomel electrode (SCE) separated from the test solution by a fine-porosity frit and an agar bridge saturated with KCl. Where possible, solutions were 5×10^{-4} mol dm^{-3} in the test compound and 0.1 mol dm^{-3} in $[NBu_4][PF_6]$ as the supporting electrolyte. At the end of each voltammetric experiment, $[Fe(\eta^5\text{-}C_5H_5)_2]$ was added to the solution as an internal standard for potential measurements. Under the conditions used, the E^o value for the $[Fe(\eta^5\text{-}C_5H_5)_2]^+/[Fe(\eta^5\text{-}C_5H_5)_2]$ couple was 0.47 V.

Caution: Powder samples of **6** and **7** explode by percussion. All attempts to isolate these compounds should be carried out with great caution.

Synthesis of $[Li(thf)_4][V^{III}(C_6Cl_5)_4]$ (1): $[VCl_3(thf)_3]$ (0.77 g, 2.06 mmol) was added at −78 °C to a solution of LiC_6Cl_5 (ca. 10 mmol) in Et_2O (60 cm^3). The suspension was allowed to warm up to 0 °C and was stirred at that temperature for about 4 h. A green solid formed, and this was filtered at 0 °C and extracted in CH_2Cl_2 (50 cm^3) at the same temperature. The solvent in the extract was replaced by thf (10 cm^3) and the slow diffusion of an Et_2O layer (40 cm^3) into it at −30 °C yielded **1** as a green solid (1.47 g, 1.09 mmol; 53% yield). IR (KBr): $\tilde{\nu}$ = 1321 (s), 1312 (s), 1284 (vs), 1224 (m), 1145 (m), 1063 (s), 1043 (s; C−O−C_{asym}),[11] 915 (sh), 887 (m; C−O−C_{sym}),[11] 829 (s; C_6Cl_5: X-sensitive vibr.),[12] 668 cm^{-1} (s); MS (FAB⁻): *m*/*z*: 1039 $[V(C_6Cl_5)_4]^-$, 827 $[V(C_6Cl_5)_3Cl]^-$, 615 $[V(C_6Cl_5)_2Cl_2]^-$, 403 $[V(C_6Cl_5)Cl_3]^-$; elemental analysis calcd (%) for $C_{40}H_{32}Cl_{20}LiO_4V$: C 35.8, H 2.4; found: C 34.8, H 2.8.

Synthesis of $[NBu_4][V^{III}(C_6Cl_5)_4]$ (1′): $[VCl_3(thf)_3]$ (2.54 g, 6.80 mmol) was added at −78 °C to a solution of LiC_6Cl_5 (ca. 55 mmol) in Et_2O (60 cm^3). The suspension was allowed to warm up to room temperature and, after 15 h of stirring, the now deep green solid was filtered, washed with Et_2O (3×5 cm^3) and extracted in CH_2Cl_2 (50 cm^3). The extract was evaporated to dryness and the resulting residue was redissolved in *i*PrOH (80 cm^3) and filtered. The addition of NBu_4Br (4.4 g, 13.6 mmol) to the filtrate caused the precipitation of a first fraction of **1′** as a deep green solid. On standing of the mother liquor at −30 °C overnight, a second crop of **1′** was obtained (45% overall yield). IR (KBr): $\tilde{\nu}$ = 1482 (m), 1458 (w), 1379 (w), 1321 (s), 1312 (s), 1283 (vs), 1224 (m), 1145 (w), 1063 (s), 1025 (w), 883 (w; NBu_4^+), 828 (s; C_6Cl_5: X-sensitive vibr.),[12] 740 (w; NBu_4^+), 669 (s), 346 cm^{-1} (w); MS (FAB⁻): *m*/*z*: 1039 $[V(C_6Cl_5)_4]^-$, 827 $[V(C_6Cl_5)_3Cl]^-$, 792 $[V(C_6Cl_5)_3]^-$, 615 $[V(C_6Cl_5)_2Cl_2]^-$, 545 $[V(C_6Cl_5)_2]^-$; Λ_M(acetone) = 108.1 S cm^2 mol^{-1}; elemental analysis calcd (%) for $C_{40}H_{36}Cl_{20}NV$: C 37.2, H 2.8, N 1.1; found: C 37.3, H 2.8, N 0.65.

Crystals suitable for X-ray diffraction analysis were obtained by slow diffusion of a layer of *i*PrOH (10 cm^3) into a solution of **1′** (20 mg) in CH_2Cl_2 (2 cm^3) at −30 °C.

Synthesis of $[Li(thf)_4][V^{III}(tcp)_4]$ (2): Complex **2** was prepared from $[VCl_3(thf)_3]$ (1.07 g, 2.86 mmol) and Li(tcp) (ca. 16 mmol) by the procedure described above for synthesising **1**. Complex **2** was obtained as a green microcrystalline solid (1.78 g, 1.67 mmol; 58% yield). IR (KBr): $\tilde{\nu}$ = 2979 (m), 2881 (m), 1551 (s), 1520 (vs), 1459 (w), 1374 (m), 1342 (vs), 1294 (w), 1238 (s), 1178 (w), 1148 (s), 1120 (m), 1092 (w), 1042 (vs; C−O−C_{asym}),[11] 915 (sh), 886 (m; C−O−C_{sym}),[11] 850 (m), 798 (vs), 773 (vs), 685 (w), 547 (m), 430 cm^{-1} (m); MS (FAB⁻): *m*/*z*: 767 $[V(C_6H_2Cl_3)_4]^-$, 623 $[V(C_6H_2Cl_3)_3Cl]^-$, 479 $[V(C_6H_2Cl_3)_2Cl_2]^-$; elemental analysis calcd (%) for $C_{40}H_{40}Cl_{12}LiO_4V$: C 45.0, H 3.8; found: C 44.5, H 3.95.

Synthesis of $[Li(thf)_4][V^{III}(dcp)_4]$ (3): Complex **3** was prepared from $[VCl_3(thf)_3]$ (1.40 g, 3.74 mmol) and Li(dcp) (ca. 22 mmol) by the procedure described above for synthesising **1** and was obtained as a green microcrystalline solid (0.54 g, 0.58 mmol; 15.5% yield). IR (KBr): $\tilde{\nu}$ = 1578 (w), 1558 (m), 1540 (s), 1462 (w), 1400 (vs), 1247 (m), 1162 (m), 1122 (s), 1091 (m), 1043 (s; C−O−C_{asym}),[11] 1012 (m), 915 (sh), 888 (m; C−O−C_{sym}),[11] 768 (s), 752 (s), 685 cm^{-1} (m); MS (FAB⁻): *m*/*z*: 631 $[V(C_6H_3Cl_2)_4]^-$, 521 $[V(C_6H_3Cl_2)_3Cl]^-$, 411 $[V(C_6H_3Cl_2)_2Cl_2]^-$, 306 $[V(C_6H_3Cl_2)(C_6H_3Cl)]^-$; elemental analysis calcd (%) for $C_{40}H_{44}Cl_8LiO_4V$: C 51.6, H 4.8; found: C 51.4, H 5.0.

Synthesis of $[V^{IV}(C_6Cl_5)_4]$ (4): Cl_2 dissolved in CCl_4 (0.62 mmol) was added at 0 °C to a solution of **1** (0.33 g, 0.25 mmol) in CH_2Cl_2 (15 cm^3). The initially green solution turned deep blue-green. After 30 min of stirring, the solution was cooled at −30 °C and allowed to stand at that temperature overnight. A blue-green solid formed, and this was filtered, washed with CH_2Cl_2 (3×3 cm^3) at −30 °C and vacuum dried (**4**·CCl_4: 0.20 g, 0.17 mmol; 68% yield). IR (KBr): $\tilde{\nu}$ = 1487 (m), 1313 (s), 1286 (vs), 1146 (s), 1132 (vs), 1072 (s), 842 (vs; C_6Cl_5: X-sensitive vibr.),[12] 782 (s), 758 (s), 678 cm^{-1} (vs); MS (FAB⁻): *m*/*z*: 1039 $[V(C_6Cl_5)_4]^-$, 827 $[V(C_6Cl_5)_3Cl]^-$, 757 $[V(C_6Cl_5)_2(C_6Cl_4)]^-$; elemental analysis calcd (%) for $C_{25}Cl_{24}V$: C 24.9; found: C 25.0.

Synthesis of $[V^{IV}(tcp)_4]$ (5): Cl_2 dissolved in CCl_4 (0.73 mmol) was added dropwise to a solution of **2** (0.65 g, 0.61 mmol) in CH_2Cl_2 (15 cm^3) at 0 °C, whereupon the initially green solution gradually turned deep blue. After 30 min of stirring, the solution was concentrated to dryness and the resulting residue was extracted in Et_2O (60 cm^3) and filtered. Evaporation of the filtrate solvent yielded a blue solid that was vacuum dried and collected (**5**·CCl_4: 0.28 g, 0.30 mmol; 50% yield). IR (KBr): $\tilde{\nu}$ = 1548 (vs), 1516 (s), 1406 (w), 1375 (w), 1345 (s), 1238 (w), 1156 (m), 1124 (s), 1101 (m), 1089 (m), 1010 (m), 851 (s), 815 (s), 784 (s), 686 (m), 662 (w), 598 (w), 552 (m), 501 (m), 432 cm^{-1} (m); MS (FAB⁻): *m*/*z*: 767 $[V(C_6H_2Cl_3)_4]^-$, 623 $[V(C_6H_2Cl_3)_3Cl]^-$, 479 $[V(C_6H_2Cl_3)_2Cl_2]^-$; elemental analysis calcd (%) for $C_{25}H_8Cl_{16}V$: C 32.4, H 0.9; found: C 31.75, H 1.25.

Synthesis of $[V^{IV}(dcp)_4]$ (6): $[N(C_6H_4Br\text{-}4)_3][SbCl_6]$ (0.23 g, 0.28 mmol) was added at 0 °C to a solution of **3** (0.52 g, 0.56 mmol) in CH_2Cl_2 (10 cm^3). The initially green solution turned deep blue. After 1 h of stirring, a deep blue solid formed. This was filtered, washed with CH_2Cl_2 (3×3 cm^3) at 0 °C and vacuum dried (**6**: 0.23 g, 0.36 mmol; 64% yield). IR (KBr): $\tilde{\nu}$ = 1652 (s), 1552 (s), 1540 (s), 1402 (vs), 1373 (s), 1247 (m), 1169 (s), 1135 (s), 1094 (s), 1062 (m), 1010 (s), 784 (m), 774 (vs), 763 (s), 692 (m), 433 (m), 389 (m), 344 cm^{-1} (m); MS (FAB⁻): no ions observed; MS (FAB⁺): no ions observed; elemental analysis calcd (%) for $C_{24}H_{12}Cl_8V$: C 45.4, H 1.9; found: C 45.3, H 1.7.

Synthesis of $[NBu_4]_2[V^{III}(C_6F_5)_5]$ (7): $[VCl_3(thf)_3]$ (1.44 g, 3.85 mmol) was added at −78 °C to a solution of LiC_6F_5 (ca. 23 mmol) in Et_2O (50 cm^3). The suspension was allowed to warm up to −30 °C and, after the addition

of NBu_4Br (1.24 g, 3.85 mmol), the temperature was further allowed to rise to 0 °C. After 3 h of stirring at this temperature, a green solid had formed; this was filtered and extracted in CH_2Cl_2 (70 cm^3) at 0 °C. The solvent in the extract was concentrated to a final volume of 20 cm^3 and the slow diffusion of an Et_2O layer (60 cm^3) into it at −30 °C yielded **7** as a microcrystalline green solid (1.67 g, 1.22 mmol; 31.6 % yield based on the vanadium precursor). IR (KBr): $\tilde{\nu}$ = 2967 (s), 2879 (m), 1628 (m), 1493 (vs), 1439 (vs), 1425 (s), 1382 (w), 1365 (w), 1325 (w), 1277 (w), 1245 (w), 1230 (w), 1173 (w), 1151 (w), 1056 (s), 1035 (s), 996 (w), 949 (vs; C_6F_5: C–F),[12] 937 (vs; C_6F_5: C–F),[12] 881 (w; NBu_4^+), 799 (w), 756 (w; C_6F_5: X-sensitive vibr.),[12] 740 (w; NBu_4^+), 711 (w), 595 (w), 482 cm^{-1} (w); MS (FAB^-): *m/z*: 905 $[V(C_6F_5)_5F]^-$, 719 $[V(C_6F_5)_4]^-$, 553 $[V(C_6F_5)_3]^-$, 386 $[V(C_6F_5)_2]^-$; elemental analysis calcd (%) for $C_{62}H_{72}F_{25}N_2V$: C 54.3, H 5.3, N 2.0; found: C 53.8, H 4.9, N 2.4.

Crystals suitable for X-ray diffraction analysis were obtained by slow diffusion of a layer of Et_2O (5 cm^3) into a solution of **7** (25 mg) in CH_2Cl_2 (1 cm^3) at −30 °C.

X-ray structure determinations: Crystal data and other details of the structure analyses are presented in Table 8. Suitable crystals of **1′** and **7** were obtained as indicated in each synthetic procedure. Crystals were mounted at the end of a glass fibre and held in place with epoxy adhesive.

Table 8. Crystal data and structure refinement for **1′** and **7**.

	1′	**7**
formula	$C_{40}H_{36}Cl_{20}NV$	$C_{62}H_{72}F_{25}N_2V$
M_r	1290.64	1371.16
T [K]	293(2)	100(2)
λ [pm]	71.073	71.073
crystal system	orthorhombic	orthorhombic
space group	*Pbca*	*Pbca*
a [pm]	1938.00(10)	2078.8(2)
b [pm]	2125.86(13)	1840.71(19)
c [pm]	2590.52(14)	3312.8(4)
V [nm^3]	10.6727(10)	12.676(2)
Z	8	8
ρ [$g\,cm^{-3}$]	1.606	1.437
μ [mm^{-1}]	1.219	0.270
$F(000)$	5168	5648
2θ range [°]	4–50 ($+h$, $+k$, $+l$)	3–50 ($\pm h$, $\pm k$, $\pm l$)
final R indices	$R_1 = 0.0589$,	$R_1 = 0.0815$,
$[I > 2\sigma(I)]$[a]	$wR_2 = 0.1128$	$wR_2 = 0.1483$
R indices (all data)	$R_1 = 0.1468$,	$R_1 = 0.1595$,
	$wR_2 = 0.1398$	$wR_2 = 0.1756$
GOF on F^2 [b]	1.011	1.042

[a] $R_1 = \Sigma(|F_o|-|F_c|)/\Sigma|F_o|$; $wR_2 = [\Sigma w(F_o^2-F_c^2)^2/\Sigma w(F_o^2)^2]^{1/2}$; $w = [\sigma^2(F_o^2) + (g_1P)^2 + g_2P]^{-1}$; $P = (1/3)\cdot[\max\{F_o^2,0\} + 2F_c^2]$. [b] Goodness-of-fit = $[\Sigma w(F_o^2-F_c^2)^2/(n_{obsd}-n_{param})]^{1/2}$.

Complex 1′: Unit-cell dimensions were determined by use of 25 centred reflections in the range $22.2 < 2\theta < 31.4°$. An absorption correction was applied on the basis of 548 azimuthal scan data (maximum and minimum relative transmission factors: 0.767 and 0.737, respectively). Reflections were collected on a Enraf–Nonius CAD4 diffractometer in an octant of reciprocal space for $4.0 < 2\theta < 50.0°$ by ω/θ scans.

Complex 7: Unit-cell dimensions were initially determined from the positions of 61 reflections in 60 intensity frames measured at 0.3° intervals in ω and subsequently refined on the basis of positions for 929 reflections from the main data set. A hemisphere of data was collected on a Bruker SMART APEX diffractometer based on three ω-scan runs (starting $\omega = -28°$) at values $\phi = 0°$, 90° and 180° with the detector at $2\theta = 28°$. For each of these runs, frames were collected at 0.3° intervals and 10 seconds per frame. An absorption correction based on 5734 symmetry equivalent reflection intensities (maximum and minimum transmission factors: 1.000 and 0.873, respectively) was applied. The diffraction frames were integrated by use of the SAINT package[52] and corrected with SADABS.[53]

The structures were solved by Patterson and Fourier methods. The refinements were carried out with the programs SHELXL-93[54] (**1′**) or SHELXL-97[55] (**7**). All non-hydrogen atoms were assigned anisotropic displacement parameters and were refined without positional constraints except as noted below. All hydrogen atoms were constrained to idealised geometries and assigned isotropic displacement parameters 1.2 times the U_{iso} value of their attached carbon atoms (1.5 times for methyl hydrogen atoms). Full-matrix, least-squares refinement of these models against F^2 converged to final residual indices given in Table 8. Lorentz and polarisation corrections were applied for all the structures.

CCDC-167901 and CCDC-256010 contain the supplementary crystallographic data for this paper. These data can be obtained free of charge from the Cambridge Crystallographic Data Centre via www.ccdc.cam.ac.uk/data_request/cif.

EPR measurements: EPR data were taken in a Bruker ESP 380 spectrometer. The magnetic field was measured with a Bruker ER035M gaussmeter. A Hewlett–Packard HP5350B frequency counter was used to determine the microwave frequency. The samples were introduced in fused quartz tubes.

Acknowledgements

This work was supported by the Spanish MCYT (DGI)/FEDER (Projects BQU2002-03997-CO2-02 and BQU2002-00554). The Gobierno de Aragón is acknowledged for a grant to M.A.G.-M. We are indebted to Prof. Dr. S. Alvarez (Universitat de Barcelona) for generously providing values of continuous shape measure.

[1] P. Berno, S. Gambarotta, D. Richeson, in *Comprehensive Organometallic Chemistry II*, *Vol. 5* (Eds.: E. W. Abel, F. G. A. Stone, G. Wilkinson), Elsevier, Oxford, U.K., **1995**, Chapter 1, pp. 1–55.

[2] P. J. Davidson, M. F. Lappert, R. Pearce, *Chem. Rev.* **1976**, *76*, 219; P. J. Davidson, M. F. Lappert, R. Pearce, *Acc. Chem. Res.* **1974**, *7*, 209.

[3] a) W. Seidel, G. Kreisel, *Z. Anorg. Allg. Chem.* **1976**, *426*, 150; b) W. Seidel, G. Kreisel, *Z. Chem.* **1976**, *16*, 115.

[4] G. Kreisel, P. Scholz, W. Seidel, *Z. Anorg. Allg. Chem.* **1980**, *460*, 51.

[5] W. Seidel, P. Scholz, G. Kreisel, *Z. Anorg. Allg. Chem.* **1979**, *458*, 263. In this paper, a coordination number higher than 4 is suggested for the V^{III} centre as the result of the *ortho*-methoxy groups becoming involved in metal coordination.

[6] Oligomeric or polymeric $[\{V(mes)_3\}_n]$ was obtained by treatment of the solvent complex $[V(mes)_3(thf)]$ with AlR_3 (R = Me, Et) under argon: R. Ferguson, E. Solari, C. Floriani, D. Osella, M. Ravera, N. Re, A. Chiesi-Villa, C. Rizzoli, *J. Am. Chem. Soc.* **1997**, *119*, 10104.

[7] G. K. Barker, M. F. Lappert, J. A. K. Howard, *J. Chem. Soc. Dalton Trans.* **1978**, 734; G. K. Barker, M. F. Lappert, *J. Organomet. Chem.* **1974**, *76*, C45.

[8] H. Köhler, P. Laub, A. Frischkorn, *J. Less-Common Met.* **1971**, *23*, 171.

[9] For a review, see: S. R. Batten, K. S. Murray, *Coord. Chem. Rev.* **2003**, *246*, 103.

[10] P. J. Alonso, J. Forniés, M. A. García-Monforte, A. Martín, B. Menjón, *Chem. Commun.* **2001**, 2138.

[11] G. M. Barrow, S. Searles, *J. Am. Chem. Soc.* **1953**, *75*, 1175; L. J. Bellamy, *The Infra-Red Spectra of Complex Molecules*, *Vol. 1*, 3rd ed., Chapman and Hall, London, **1975**, Chapter 7, pp. 129–140.

[12] a) R. Usón, J. Forniés, *Adv. Organomet. Chem.* **1988**, *28*, 219; b) E. Maslowsky, Jr., *Vibrational Spectra of Organometallic Compounds*, Wiley, New York, **1977**, pp. 437–442.

[13] W. J. Geary, *Coord. Chem. Rev.* **1971**, *7*, 81.

[14] I. Ara, J. Forniés, M. A. García-Monforte, A. Martín, B. Menjón, *Chem. Eur. J.* **2004**, *10*, 4186.
[15] G. L. Heard, R. J. Gillespie, D. W. H. Rankin, *J. Mol. Struct.* **2000**, *520*, 237. R. J. Gillespie, P. L. A. Popelier, *Chemical Bonding and Molecular Geometry*, Oxford University Press, New York, **2001**, Section 5.9, pp. 130–132.
[16] For the definition of the continuous shape measure (*S*) and its use for accurately describing coordination entities in terms of the most usual polyhedra, see: M. Pinsky, D. Avnir, *Inorg. Chem.* **1998**, *37*, 5575; J. Cirera, P. Alemany, S. Alvarez, *Chem. Eur. J.* **2004**, *10*, 190; D. Casanova, P. Alemany, J. M. Bofill, S. Alvarez, *Chem. Eur. J.* **2003**, *9*, 1281; S. Alvarez, D. Avnir, M. Llunell, M. Pinsky, *New J. Chem.* **2002**, *26*, 996; S. Alvarez, M. Llunell, *J. Chem. Soc. Dalton Trans.* **2000**, 3288.
[17] M. Llunell, D. Casanova, J. Cirera, J. M. Bofill, P. Alemany, S. Alvarez, M. Pinsky, D. Avnir, SHAPE (Version 1.1), Universitat de Barcelona (Spain) and the Hebrew University of Jerusalem (Israel).
[18] P. J. Alonso, J. Forniés, M. A. García-Monforte, A. Martín, B. Menjón, *Chem. Commun.* **2002**, 728; see also Ref. [14].
[19] T. Głowiak, R. Grobelny, B. Jeżowska-Trzeblatowska, G. Kreisel, W. Seidel, E. Uhlig, *J. Organomet. Chem.* **1978**, *155*, 39.
[20] a) P. J. Alonso, J. Forniés, M. A. García-Monforte, A. Martín, B. Menjón, C. Rillo, *Chem. Eur. J.* **2002**, *8*, 4056; b) P. J. Alonso, L. R. Falvello, J. Forniés, M. A. García-Monforte, A. Martín, B. Menjón, G. Rodríguez, *Chem. Commun.* **1998**, 1721.
[21] M. P. García, M. V. Jiménez, A. Cuesta, C. Siurana, L. A. Oro, F. J. Lahoz, J. A. López, M. P. Catalán, A. Tiripicchio, M. Lanfranchi, *Organometallics* **1997**, *16*, 1026.
[22] J. Forniés, B. Menjón, R. M. Sanz-Carrillo, M. Tomás, N. G. Connelly, J. G. Crossley, A. G. Orpen, *J. Am. Chem. Soc.* **1995**, *117*, 4295.
[23] M. M. Zaripov, V. S. Kropotov, L. P. Livanova, V. A. Stepanov, *Phys. Solid State* **1968**, *9*, 2346; M. M. Zaripov, V. S. Kropotov, L. P. Livanova, V. A. Stepanov, *Phys. Solid State* **1968**, *10*, 262.
[24] J. C. Launay, T. Arnoux, H. J. von Bardeleben, *Semicond. Sci. Technol.* **1997**, *12*, 47; R. N. Schwartz, M. Ziari, S. Trivedi, *Phys. Rev. B* **1994**, *49*, 5274, and references given therein.
[25] J. Krzystek, A. T. Fiedler, J. J. Sokol, A. Ozarowski, S. A. Zvyagin, T. C. Brunold, J. R. Long, L.-C. Brunel, J. Telser, *Inorg. Chem.* **2004**, *43*, 5645; P. L. W. Tregenna-Piggott, S. P. Best, H. U. Güdel, H. Weihe, C. C. Wilson, *J. Solid State Chem.* **1999**, *145*, 460; P. L. W. Tregenna-Piggott, H. Weihe, J. Bendix, A.-L. Barra, H.-U. Güdel, *Inorg. Chem.* **1999**, *38*, 5928.
[26] An account concerning the magnetic properties of the pseudo-metallocene cationic complex $[V(\eta^5\text{-}C_5H_5)\{HB(pz)_3\text{-}\kappa^3N)\}]^+$ has also appeared: T. J. Brunker, J. C. Green, D. O'Hare, *Inorg. Chem.* **2003**, *42*, 4366. The X-band EPR data reported there, however, seem to be inconsistent with those authors' own magnetic-susceptibility measurements. From the low-temperature behaviour of the magnetic susceptibility, a very large ZFS effect can be inferred, which would preclude the observation of a defined X-band EPR spectrum. Moreover, the spectral parameters reported are perfectly compatible with a V^{IV} (d^1) centre, a possibility that should be carefully checked by quantification of the observed signal. Precedents for the observation of V^{IV} species while studying V^{III} compounds by EPR spectroscopy already exist: F. A. Cotton, J. Lu, *Inorg. Chem.* **1995**, *34*, 2639; see also later on in the current work.
[27] A. Abragam, B. Bleaney, *Electron Paramagnetic Resonance of Transition Ions*, Clarendon, Oxford, U.K., **1970**.
[28] The electronic absorption spectrum obtained for $[Li(thf)_4][V^{III}(mes)_4]$ is similar to that reported in Ref. [3a] except for the highest energy transition, for which we observed an absorption centred at 23460 cm^{-1} in contrast with the value given in the referred work (22700 cm^{-1}).
[29] D. J. Newman, W. Urban, *Adv. Phys.* **1975**, *24*, 793; D. J. Newman, *Adv. Phys.* **1971**, *20*, 197.
[30] R. Usón, J. Forniés, M. Tomás, B. Menjón, R. Bau, K. Sünkel, E. Kuwabara, *Organometallics* **1986**, *5*, 1576; R. Usón, J. Forniés, M. Tomás, B. Menjón, K. Sünkel, R. Bau, *J. Chem. Soc. Chem. Commun.* **1984**, 751; see also Ref. [22].
[31] W. Ludwig, W. Seidel, *Thermochim. Acta* **1985**, *85*, 59; see also Ref. [3b].
[32] The fact that only half of the theoretically required amount of oxidant, $[N(C_6H_4Br\text{-}4)_3][SbCl_6]$, was needed in the synthesis of **6** can be attributed to the documented ability of the $[SbCl_6]^-$ anion also to become involved in oxidation processes. See: F. A. Cotton, S. C. Haefner, A. P. Sattelberger, *Inorg. Chim. Acta* **1998**, *271*, 187; R. Rathore, A. S. Kumar, S. V. Lindeman, J. K. Kochi, *J. Org. Chem.* **1998**, *63*, 5847; R. Rathore, J. K. Kochi, *J. Org. Chem.* **1995**, *60*, 4399; G. W. Cowell, A. Ledwith, A. C. White, H. J. Woods, *J. Chem. Soc. B* **1970**, 227.
[33] K. J. R. Rosman, P. D. P. Taylor, *Pure Appl. Chem.* **1998**, *70*, 217.
[34] J. E. Wertz, J. R. Bolton, *Electron Paramagnetic Resonance: Elementary Theory and Practical Applications*, McGraw Hill, New York, **1972**, p. 287.
[35] T. M. Dunn, *Trans. Faraday Soc.* **1961**, *57*, 1441.
[36] C. E. Holloway, F. E. Mabbs, W. R. Smail, *J. Chem. Soc. A* **1968**, 2980.
[37] G. F. Kokoszka, H. C. Allen, Jr., G. Gordon, *Inorg. Chem.* **1966**, *5*, 91.
[38] R. Kirmse, J. Stach, G. Kreisel, *J. Organomet. Chem.* **1981**, *210*, 73.
[39] D. D. Heinrich, K. Folting, J. C. Huffman, J. G. Reynolds, G. Christou, *Inorg. Chem.* **1991**, *30*, 300.
[40] E. Clementi, C. Roetti, *At. Data Nucl. Data Tables* **1974**, *14*, 177.
[41] P. J. Alonso, L. R. Falvello, J. Forniés, M. A. García-Monforte, B. Menjón, *Angew. Chem.* **2004**, *116*, 5337; *Angew. Chem. Int. Ed.* **2004**, *43*, 5225.
[42] P. J. Alonso, J. Forniés, M. A. García-Monforte, A. Martín, B. Menjón, *Organometallics* **2005**, *24*, 1269.
[43] A. R. Rossi, R. Hoffmann, *Inorg. Chem.* **1975**, *14*, 365.
[44] H. A. Jahn, E. Teller, *Proc. R. Soc. London Ser. A* **1937**, *161*, 220.
[45] W. A. Sheppard, *J. Am. Chem. Soc.* **1970**, *92*, 5419.
[46] A. Gavezzotti, in *Structure Correlation*, *Vol. 2* (Eds.: H.-B. Bürgi, J. D. Dunitz), VCH, Weinheim, **1994**, Chapter 12, pp. 509–542.
[47] B. Heyn, B. Hipler, G. Kreisel, H. Schreer, D. Walther, *Anorganische Synthesechemie*, 2nd ed., Springer, Berlin, **1990**, pp. 18–19.
[48] F. Mongin, E. Marzi, M. Schlosser, *Eur. J. Org. Chem.* **2001**, 2771.
[49] R. Usón, A. Laguna in *Inorganic Syntheses*, *Vol. 21* (Ed.: J. P. Fackler, Jr.), Wiley, New York, **1982**, Section 15.B, p. 72.
[50] M. D. Rausch, F. E. Tibbets, H. B. Gordon, *J. Organomet. Chem.* **1966**, *5*, 493.
[51] F. Bermejo, *Tratado de Química Analítica*, 6th ed., Editorial Dossat, Madrid, **1981**, p. 813.
[52] SAINT, Version 5.0, Bruker Analytical X-ray Systems, Madison WI.
[53] G. M. Sheldrick, SADABS empirical absorption program, Version 2.03, University of Göttingen, Göttingen, Germany, **1996**.
[54] G. M. Sheldrick, SHELXL-93, Program for the Refinement of Crystal Structures from Diffraction Data, University of Göttingen, Göttingen, Germany, **1993**.
[55] G. M. Sheldrick, SHELXL-97, Program for the Refinement of Crystal Structures from Diffraction Data, University of Göttingen, Göttingen, Germany, **1997**.

Received: November 22, 2004
Published online: May 25, 2005